Reliability-Based Thermal and Wind Units Economic Dispatch in Presence of DSRP

Farzad Arefi[1], Hassan Meyar-Naimi[2*] and Ahmad Ghaderi Shamim[3]

[1] Department of Electrical Engineering, Hamedan branch, Islamic Azad University, Hamedan, Iran
Farzad_are2000@yahoo.com

[2] Department of Electrical Engineering, Hamedan branch, Islamic Azad University, Hamedan, Iran.
h.meyar.naimi@gmail.com

[3] Department of Electrical Engineering, Hamedan branch, Islamic Azad University, Hamedan, Iran.
ahmadghaderi@yahoo.com

***Abstract*--**Recently, Wind Turbines (WTs) and Electric Vehicles (EVs) have been integrated into the demand side of many countries. WTs and EVs have uncertainties in electrical energy generation and consumption, respectively. Additionally, Thermal Units (TUs) suffer from random failures. As always, secure power system operation is the main goal of an independent system operator, therefore, these uncertainties should be considered. This paper proposes a two-stage reliability-based model for the economic dispatch of TUs and WTs in the presence of a demand-side response program. At the first stage, the well-being analysis is performed to determine the power generation and spinning reserve of the TUs regarding the timely power generation of WTs. At the second stage, the adoption of the responsive load consumption with the various conditions of the generation system in the power pool market is established using the cost of expected energy not served criterion. This optimization problem is solved at two stages using the genetic algorithm. To validate the proposed model, numerical studies have been applied to the generation part of an IEEE test power system including eleven TUs, one WT, and one thousand EVs.

***Index Terms*--**Generation System Economic Dispatch, Uncertainties, Well-Being Analysis (WBA), Wind Turbines (WTs), Electric Vehicles (EVs), and Demand Side Response Program (DSRP).

I. INTRODUCTION

Power systems experience a variable daily load demand from low loads to peak loads due to changes in customers' energy consumption tendencies. In restructured power systems, the Independent System Operator (ISO) should optimally dispatch the total load demand on available Thermal Units (TUs) in the power market, while, TU's technical constraints and network limits should be satisfied, and the timely power generation of wind turbines (WTs) must be estimated [1]. Because of the growing need for energy resources, fossil fuel reduction, carbon emissions, and other limitations, the participation of WTs in the generation systems is more necessary than in previous years. Many countries have planned to increase the penetration of WTs into their power systems due to more availability and efficiency [2]. The output power of WT is often uncertain since wind speed is not exactly predictable during the day [3]. To overcome this problem, so far, various solutions have been suggested, including the use of dispatchable resources such as energy storage systems and TUs with complementary performance for WTs [4]-[5]-[6], reserve provision [7]-[8], and the use of the Demand-Side Response Program (DSRP) [9]. Energy storage systems are expensive, and TUs cause carbon emissions and high operating and maintenance costs. But, reserve provision on TUs and DSRP through responsive loads (RLs) are two affordable methods. First, DSRP has been used for many years to refer to peak load shaving while it is limited to several hours per year [9]-[10]. Thus, incentive-based and reliability-based DSRPs are widely implemented in different countries. The first case provides mutual economic signals to meet the load demand. But, the second case operates under emergency conditions [11]. The ISO can smooth the output power of WTs using DSRP, especially using EVs [12]. EVs with other RLs will play an important role in facilitating and increasing the participation of WTs in the day-ahead power market [13]. Therefore, up to now, many kinds of research have been conducted: In [14], impacts of the joint operation of WT power producers with EVs and other RLs have perused as a virtual power plant in electricity markets. In [15], EVs-WTs coordinated scheduling is applied to improve uncertain wind power adsorption. A profit-based unit commitment of TUs with renewable energy and EVs has been presented in [16]. In [17], DSRP is applied in industrial energy management considering thermostatically controlled loads and EVs. Often, in the operation planning process, there are some uncertainties such as single contingencies of TUs, the output power of WTs, and the charging-discharging of EVs. The operating reserve is determined using deterministic, probabilistic, and well-being methods [18]. The probabilistic method determines the system operating reserve using risk or reliability indices such as loss of load probability, expected energy not served, loss of load frequency, and loss of load duration [19]. The optimal amount of the system risk at each hierarchical level sets the operating reserve. But, Well-Being Analysis (WBA) combines deterministic and probabilistic methods to set the operating reserve [20]. In WBA, the power system is in a health, margin, or risk state. It is in a healthy state when the reserve capacity is sufficient to satisfy the predefined reliability criteria. It is in a marginal state when the reserve capacity is only sufficient to supply load, but it fails to satisfy the predefined reliability criteria. It is in a risk state when the reserve capacity isn't adequate to supply the load. The power system state can change between them dynamically. Despite the

performance improvement of power systems by this method, in recent years, little research has been done in this area. For example, WBA is applied to the system state identification by making the capacity outage probability table for TUs considering the participation of WTs [21] and EVs [22]. In [23], an analytical technique has been introduced to model three probabilistic indices of WBA including the health, margin, and risk probabilities, and also its application in the preventive maintenance scheduling of generating facilities. Bulk electric system WBA using sequential Monte Carlo simulation was established in [24]. In [25], a WBA-based approach to assessing the health of the bulk power system by incorporating fuzzy sets has been suggested. An analytical approach for WBA of small autonomous power systems with solar and wind energy sources is proposed in [26]. In [27], WBA is applied for wind-integrated power systems. WBA of generating systems considering charging of EVs has been modeled in [28]. In [29], the impacts of increasing deployment of GT units in power system operation are studied and evaluated using WBA. In this investigation, WBA is conducted considering the uncertainties of system operation states and renewable energy sources. As can be obtained from the literature review, despite its efficiency, the WBA tool has been very little applied in power systems. In the previous investigations, the correct model of EV is not used for solving the economic dispatch (ED) problem. Operation uncertainties including single contingencies of TUs, charging/discharging of EVs, and variable output of WTs have not been considered simultaneously. Their solution algorithm was not efficient enough to calculate the global optimal solution. Therefore, this paper proposes a two-stage model for load ED on TUs in the presence of WTs and EVs. At the first stage, the Well-Being analysis determines the amount of power generation and spinning reserve (SR) for TUs based on the timely prediction of WTs output power. At the second stage, the consumption profile of RLs based on the generation system conditions in the power pool market is determined using the cost of expected energy not served criterion. The mentioned optimization problem in each stage is solved using the genetic algorithm. The rest of the paper is organized as follows: In section2, the Auto recursive and moving average (ARMA) time series is used to model the operation of WTs. Section3 will model the operation of EV and DSRP. The proposed flowchart comes in section 4. To validate the proposed two-stage model, numerical studies are performed on a test network in section 5. In section 6, our simulation results are compared with other works. The conceptual results are gathered in section 7.

II. ARMA FOR WTS MODELLING

The WTs output power completely depends on the wind regime and the specifications of the generator, and it can be determined in each hour with the ARMA time series model using the region's historical weather data for ten or twenty years according to equations (1), and (2).

$$y_t = 1.772y_{t-1} + 0.1001y_{t-2} - 0.3572y_{t-3} + 0.0379y_{t-4} + \alpha_t \\ -0.5030\alpha_{t-1} - 0.2924\alpha_{t-2} + 0.1317\alpha_{t-3} \quad (1)$$

$$SW_t = \mu_t + \sigma_t y_t \quad (2)$$

If, ARMA(4,3) is considered as a time series according to relation (1) for a specific region. The index α_t is a normal white noise process with average and variance equal to 0 and 0.524760^2, respectively. WT's wind speed (SW_t) is calculated according to relation (2). Indexes σ_t and μ_t are defined as standard deviation and the average values of wind speed in hour t. Simulation ARMA(4,3) for wind speed estimation ultimately leads to a probabilistic distribution, which can determine WT's output power as a function of the predicted wind speed according to the relation (3). The output power of WTs is determined through their operation parameters (V_{ci}, V_{co} and V_r), and nominal output power (P_r) [27]. Parameters A, B, and C can be calculated based on wind speed operation parameters according to relation (4), (5), and (6), respectively. Here, the output power of WTs is assumed as negative power absorption.

$$PP(SW_t) = \begin{cases} 0, & 0 \le SW_t \le V_{ci} \\ A + (B \times SW_t) + (C \times SW_t^2) \times P_r & V_{ci} \le SW_t \le V_r \\ P_r, & V_r \le SW_t \le V_{co} \\ 0, & SW_t \ge V_{co} \end{cases} \quad (3)$$

$$A = \frac{1}{(V_{ci} - V_r)^2} \left\{ V_{ci}(V_{ci} + V_r) - 4V_{ci}V_r \left[\frac{V_{ci} + V_r}{2V_r} \right]^3 \right\} \quad (4)$$

$$B = \frac{1}{(V_{ci} - V_r)^2} \left\{ 4(V_{ci} + V_r) \left[\frac{V_{ci} + V_r}{2V_r} \right]^3 - (3V_{ci} + V_r) \right\} \quad (5)$$

$$C = \frac{1}{(V_{ci} - V_r)^2} \left\{ 2 - 4 \left[\frac{V_{ci} + V_r}{2V_r} \right]^3 \right\} \quad (6)$$

A comparison of historical data for several decades shows that ARMA(4,3) produces reasonable and acceptable results for wind speed even in the presence of measurement noise, therefore, it is used for the operation modeling of WTs.

III. MODELLING OF DSRP AND EV

A. DSRP

The DSRP refers to all actions during the days, weeks, and seasons of the year to make desirable changes in various industrial, commercial, residential, and agricultural customer time-consumption patterns, which cause higher reliability and greater social welfare for customers at a lower cost. Often, desirable changes in time-consumption patterns consist of peak clipping, valley filling, load shifting, etc. To model the DSRP, load aggregators receive the price-power consumption and utilization limits. RLs offer contains several power-price blocks, in which load increases lead to a decrease in the price of consumption. RLs can cut off or shift their load demand to another time to satisfy the system's economic and reliability constraints. Thus, the demand curve includes the constant load, expected load, maximum load, and step response sections according to Figure (1). In the bellow curve, OA, OC, OD, and BC represent the constant loads of CBL, the expected hourly load, the maximum hourly load, and the minimum load curtailment [25]. The fixed loads in different hours are price-taker, which are settled at the energy price, OE represents the

actual customer load scheduled in the day-ahead power market by ISO. The adjustable load $DR_{b,t}$ is the difference between the expected and scheduled load. It is positive for the load cutoff condition, negative for the load shift condition, and zero for the no-shift or load cutoff condition. Equation (7) shows that TUs and WTs supply the scheduled load demand. The scheduled load is equal to the fixed loads plus the sum of the responsive loads in the n blocks as Equation (8).

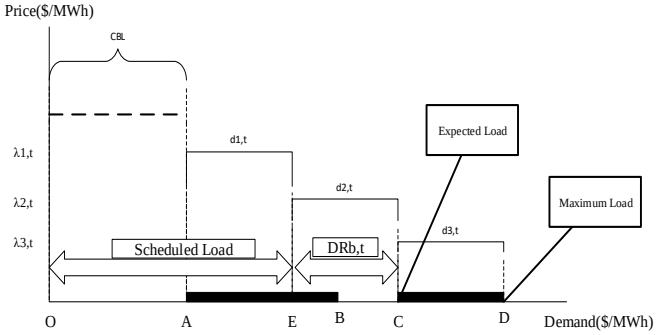

Figure (1): load demand curve includes the constant, expected, and maximum load demand and the step response section

$$\sum_{i=1}^{N_{th}} PG_i^t + \sum_{j=1}^{N_{WT}} PW_j^t = PD_t - DR_{b,t} \tag{7}$$

$$CBL_t + \sum_{n=1}^{NB} d_{n,t} = PD_t - DR_t \quad \forall t \in T \tag{8}$$

The maximum amount of power in each block is as Equation (9). The physical constraint of the adjustable load is described by Equations (10) and (11). The index I_t^D is the binary variable that indicates the load state at time t, it will be 1 when the state is changed and 0 otherwise.

$$0 \le d_{n,t} \le d^{MAX}{}_{n,t} \quad \forall t \in T, \forall n \in NB \tag{9}$$

$$CL^{\min} \times I_t^D \le DR_t \le CL^{\max}{}_t \times I_t^D \tag{10}$$

$$if \quad DR_t \ge 0 \quad \forall t \in T$$

$$DR_t \ge PD_t - PD_t^{\max} \quad if \quad DR_t \prec 0 \quad \forall t \in T \tag{11}$$

B. Modelling of EVs

EVs can play an important role in increasing the participation of WTs in the generation system. They can adjust their consumption according to different generation conditions and even provide other services such as reserve capacity for the system [24]. The EVs in the parking and network connection state can be charged (CCH=2) and discharged (CDCH=3) with different efficiencies. In parking and non-connection to the grid state (DP=1), energy losses are equal to zero. In the road driving mode of EVs (DM=4), although the efficiency of EVs energy conversion from the battery to the wheels is different from other modes, the energy consumption will depend on the distance and time pattern. The energy conversion efficiency divides into charging and connection to grid mode (eff_{EVs}^{CCH}), discharging and connection to grid mode (eff_{EVs}^{CDCH}), and discharging and moving on the road (eff_{EVs}^{DM}). The EVs operation model must consider all main factors such as charge status at the beginning of the day, the hourly use and connection profile to the grid, maximum and minimum battery charge status, the charge and discharge rates, and maximum power output. The charging and discharging of all types of EVs are intelligent and managed by demand-side aggregators so that they can respond to the electricity market price. The EV owners decide on their driving pattern when ISO chooses how to charge and discharge the batteries to optimize the electricity market financial issue while permitting more penetration of WT resources. Stored energy in different types of EV batteries is a function of the energy stored in the previous time interval, the amount of charging and discharging power from/to the grid in the current time interval, and moving time and distance on the roads without connection to the distribution network. EV battery discharges and gives energy to the wheels in the current time interval as Equation (12).

$$\left\{ \begin{array}{l} SoC_{EVs}^t = SoC_{EVs}^{t-1} + (PB_{EVs}^{CCH,t} \times eff_{EVs}^{CCH}) - (\dfrac{PB_{EVs}^{CDCH,t}}{eff_{EVs}^{CDCH}}) - (\dfrac{ET_{EVs}^{DM}}{eff_{EVs}^{DM}}) \\ BOS_{EVs}^{s,t} \rightarrow \begin{cases} s \in CCH, CDCH, DM, DP \\ EVs \in Cars, Vans, Trucks \end{cases} \end{array} \right\} \tag{12}$$

The index ET_{EVs}^{DM} is the amount of energy discharged from the battery of the EV in the moving state during time interval t in terms of MWh. Indexes $PB_{EVs}^{CCH,t}$ and $PB_{EVs}^{CDCH,t}$ are the power consumption/generation of EV battery in grid-connected mode during time interval t. Index SoC_{EVs}^t is the amount of stored energy in the battery of an EV at the end of time interval t. Therefore, batteries of each type of EVs are placed in one of four operating states during time interval t as Equation (13).

$$\sum_{s \in \{CCH, CDCH, DM, DP\}} BOS_{EVs}^{s,t} = 1 \qquad \forall EVs \in Cars, Vans, Trucks \tag{13}$$

The index $BOS_{EVs}^{s,t}$ is the binary variable indicates that the operating status of the EV battery for time interval t. The energy loss is zero for the EV battery in the park status without a grid connection. In addition, stored energy in the EV battery for the end of time interval t will be equal to the starting time interval. As Equation (14), the amount of power injected/consumed by the EV battery to/from the grid in the connection state for the time interval t cannot be less/more than the minimum/maximum capacity limit. The change in charge and discharge status during two consecutive operation planning time intervals should not exceed than allowable rate as Equations (15) and (16).

$$BSC_{EVs}^{\min} \le SoC_{EVs}^t \le BSC_{EVs}^{\max} \tag{14}$$

$$SoC_{EVs}^t - SoC_{EVs}^{t-1} \le ER_{EVs}^{Up}$$
$$\forall s \in CCH \quad and \quad \forall EVs \in Cars, Vans, Trucks \tag{15}$$

$$SoC_{EVs}^{t-1} - SoC_{EVs}^t \le ER_{EVs}^{Down}$$
$$\forall s \in CDCH, DM \quad and \quad \forall EVs \in Cars, Vans, Trucks \tag{16}$$

The indexes ER_{EVs}^{Up} / ER_{EVs}^{Down} are the charge/discharge rate of

the EV battery. The indexes $BSC_{EVs}^{\max}/BSC_{EVs}^{\min}$ are the maximum/minimum storage capacity of the EV battery.

IV. Proposed Flowchart for Thermal-Wind Units ED in the Presence of DSMP

This section describes the proposed flowchart to solve the optimization problem of load ED on TUs in the presence of WTs and EVs and also other RLs. We should code mentioned problem into the genetic algorithm to achieve an optimal solution. The Objective Function (OF) in the first stage is the minimization of the total cost of fuel consumption and SR provision by TUs. Constraints are the technical limits of TUs and WTs. Independent variables are the production of TUs based on the estimation of power generation of WTs and their SR. OF in the second stage is profit maximization for all participants in the power market, especially EVs. Constraints are the technical limits of residential, commercial, industrial, and agricultural loads and EVs. In the second stage, Independent variables are the participation level of all types of RLs. After the problem solution in the first stage, output results enter the second stage as input data. Figure (2) shows our solution flowchart.

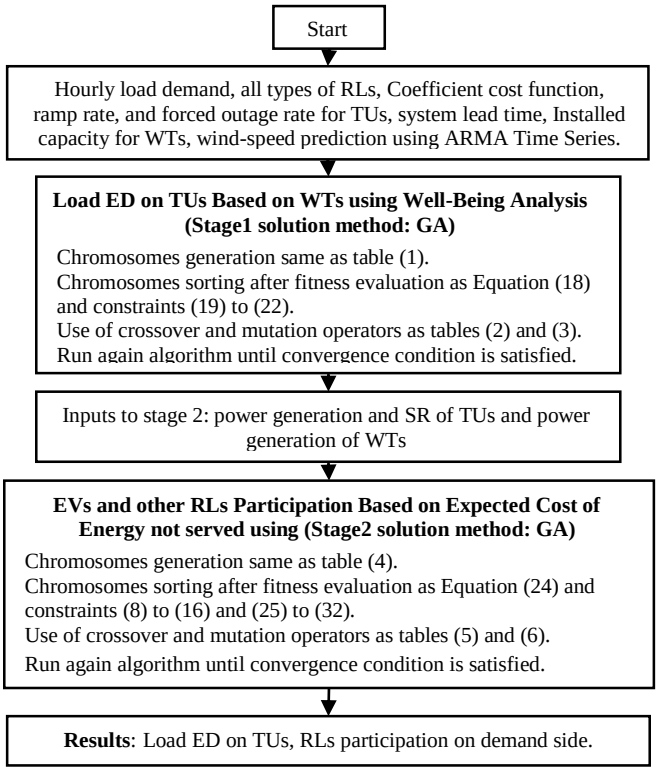

Figure (2): Proposed Flowchart for ED on TUs in presence of WTs and RLs

First, cost function coefficients, minimum and maximum power generation, ramp-up and down rates, failure and repair rates of TUs and system lead time, WTs capacity, wind speed-power prediction using the ARMA time series model, expected load in the electricity market, desired level of system risk and health as known information should enter into the model as input data. Then, the genetic algorithm solves the model at the first stage. The chromosome population is equal to a problem solution according to Table (1) and OF in stage1 is as Equation (17).

Table (1): a chromosome equal to the problem solution at the first stage

PG_1^t	.	$PG_{N_{th}}^t$	SR_1^t	..	$SR_{N_{th}}^t$	PW_1^t	..	$PW_{N_{WT}}^t$

$$OF_{Stage1}^{Model} = Min\left(\sum_{t=1}^{24}\sum_{i=1}^{N_{th}} OC_i^t + SRC_i^t\right) \rightarrow \begin{Bmatrix} OC_i^t = \alpha_i + \beta_i PG_i^t + \gamma_i PG_i^{t\,2} \\ SRC_i^t = SR_{price_i}^t \times SR_i^t \end{Bmatrix} \quad (17)$$

Indices PG_i^t and OC_i^t are power production of TUs and corresponding fuel cost in time t, respectively. Indices α_i, β_i and γ_i are coefficients of the cost function. The index N_{th} is the number of TUs. Indices SR_i^t and $SR_{price_i}^t$ are the amount and price of SR to provide the desired level of system risk and general health in time t. Based on (17), the fitness of each chromosome can be defined as Equation (18).

$$fitness_{Stage1} = OF_{Stage1}^{Model} + Penalty_{Stage1}^{total} \quad (18)$$

The technical constraints include minimum and maximum power generation of TUs as Equation (19), maximum power generation of WTs as Equation (20), availability of sufficient capacity to meet the expected demand of customers as Equation (21), and availability of sufficient reserve capacity for providing desired system risk and health as Equation (22).

$$PG_i^{\min} \le PG_i^t \le PG_i^{\max} \quad (19)$$

$$PW_i^t \le PW_i^{\max} \quad (20)$$

$$\sum_{i=1}^{N_{th}} PG_i^t + \sum_{j=1}^{N_{WT}} PW_j^t \ge PD_t \quad (21)$$

$$\sum_{i=1}^{N_{th}} SR_i^t \ge SR_t \rightarrow \left\{\Pr_{RGS} \le A_R, \text{and } \Pr_{HGS} \ge A_H\right\} \quad (22)$$

A penalty imposes on fitness function due to any violation of constraints. Therefore, the sub-optimal solution is automatically removed from the solution space. Indices A_R and A_H are the acceptable level of system risk and general health of the generation system. Indices $\Pr_{RGS}$ and $\Pr_{HGS}$ are the probability of risk and general health of the generation system, respectively. Crossover occurs for each two-parent chromosome, and a pair of child chromosomes will produce according to Table (2). Then, the mutation operator changes a child's chromosome shown in Table (3).

Table (2): Intersection operator for two-parent chromosomes to produce a pair of child chromosomes at the first stage of the proposed model

PG_1^t	..	$PG_{N_{th}}^t$	SR_1^t	...	$SR_{N_{th}}^t$	PW_1^t	..	$PW_{N_{WT}}^t$
PG''^t_1	..	$PG''^t_{N_{th}}$	SR''^t_1	...	$SR''^t_{N_{th}}$	PW''^t_1	..	$PW''^t_{N_{WT}}$
		↓						↓
PG''^t_1	..	$PG''^t_{N_{th}}$	SR_1^t	...	$SR_{N_{th}}^t$	PW_1^t	..	$PW_{N_{WT}}^t$
PG''^t_1	..	$PG''^t_{N_{th}}$	SR''^t_1	...	$SR''^t_{N_{th}}$	PW_1^t	..	$PW_{N_{WT}}^t$

After the parent's crossover into the mating pool and child mutation, a new population sorts based on fitness evaluation, and the next iteration starts again until a convergence condition is satisfied.

Table (3): mutation operator in the first child chromosome at the first stage

PG''^{t}_{1}	..	$PG''^{t}_{N_{th}}$	SR^{t}_{1}	...	$SR^{t}_{N_{th}}$	PW^{t}_{1}	..	$PW^{t}_{N_{WT}}$
					↓			
PG''^{t}_{1}	..	$PG''^{t}_{N_{th}}$	SR^{t}_{1}	..	$SR'^{t}_{N_{th}}$	PW^{t}_{1}	..	$PW^{t}_{N_{WT}}$

Second-stage inputs are first-stage output results such as TU's power generation and SR, and also the power generation of WTs. The chromosome structure for problem solution in the second stage includes the state of charge for batteries of EVs and other RLs participation in the power market following Table (4).

Table (4): chromosome structure for problem solution in the second stage

SoC^{t}_{EV1}	SoC^{t}_{EV2}	.	SoC^{t}_{EVm}	DR^{t}_{Res}	DR^{t}_{Com}	DR^{t}_{Ind}	DR^{t}_{Agr}

The index SoC^{t}_{EVi} is the stored energy in the battery of the EV in time interval t. Indices $DR^{t}_{\text{Res}}, DR^{t}_{Com}, DR^{t}_{Ind}$, and DR^{t}_{Agr} are the participation of RLs including residential, commercial, industrial, and agricultural consumers in time interval t. When an EV is present in the parking lot, the amount of injected power ($PB^{CDCH,t}_{EVs}$)/absorption power ($PB^{CCH,t}_{EVs}$) into/from the power network can be calculated using the amount of stored energy in the battery in time interval t according to Equations (12) to (16). Here, OF in stage2 is as Equation (23).

$$OF^{Model}_{level\,2} = Max(\sum_{t=1}^{24}\sum_{i=1}^{N_{EVs}}(PB^{CDCH,t}_{EVi} - PB^{CCH,t}_{EVi}) \times E^{t}_{\text{Price}} + \sum_{t=1}^{24}\sum_{j=1}^{N_{DRs}}(DR^{pos}{}_{t} + DR^{neg}{}_{t}) \times E^{Inc}_{price}) \quad (23)$$

Based on the OF according to Equation (23), the fitness of each chromosome is defined as Equation (24). The generation and load balance limit is according to Equation (24). The participation levels of RLs are according to Equations (25) and (26), respectively. The violation of technical constraints from (7) to (16) will impose a penalty on fitness function in the second stage.

$$fitness_{level\,2} = \frac{OF^{Model}_{level\,2}}{1 + Penalty^{total}_{level\,2}} \quad (24)$$

$$\sum_{i=1}^{N_{th}} PG^{t}_{i} + \sum_{j=1}^{N_{WT}} PW^{t}_{j} + \sum_{i=1}^{N_{EVs}} PB^{CDCH,t}_{EVi} = (PD_{t} + \sum_{i=1}^{N_{EVs}} PB^{CCH,t}_{EVi}) - DR_{t} \quad (25)$$

$$DR_{t} = DR^{pos}{}_{t} \times u^{pos}{}_{t} + DR^{neg}{}_{t} \times u^{neg}{}_{t}$$
$$\rightarrow \{DR^{t}{}_{\text{Res}}, DR^{t}{}_{Com}, DR^{t}{}_{Inv}, DR^{t}{}_{Agr}\} \in DR_{t} \quad (26)$$
$$u^{pos}{}_{t} + u^{neg}{}_{t} \le 1$$

In the second-stage model, available SR on TUs (SR^{Ava}_{i}) computes considering the ramp rate of TUs and participation of EVs and other RLs according to Equation (27). The probability of a TU's unavailability considering single contingencies is according to Equation (28). The probabilistic tree method generates the generation scenarios of WTs based on their probability distribution function according to Equation (29). Often, load shedding is occurred due to a lack of generation capacity after SR activation and participation of RLs in each abnormal condition as Equation (30).

$$SR^{Ava,t}_{i} = Min(RR_{i}, SR^{t}{}_{i}) \quad (27)$$

$$\Pr^{O,t}_{k} = ORR^{O,t}_{k} \prod_{h=i(i\neq k)} (1 - ORR^{O,t}_{i}) \quad (28)$$

$$SC_{WTj} = \{(P_{WTj}{}^{sc1}, \rho r_{WTj}{}^{sc1}), (P_{WTj}{}^{sc2}, \rho r_{WTj}{}^{sc2}), ...(P_{WTj}{}^{Sc_n}, \rho r_{WTj}{}^{Sc_n})\}$$
$$\sum_{i=1}^{Sc_n} \rho r_{WTj}{}^{Sci} = 1 \quad (29)$$

$$PL^{t}_{sh}(k,sc) = (\sum_{\substack{i=1 \\ i\neq k}}^{N_{th}} (PG^{t}_{i} + SR^{Ava,t}_{i}) + \sum_{j=1}^{N_{WT}} P^{Sc,t}_{WTj} + \sum_{i=1}^{N_{EVs}} PB^{CDCH,t}_{EVi}) - (PD_{t} + \sum_{i=1}^{N_{EVs}} PB^{CCH,t}_{EVi}) - DR_{t} \quad (30)$$

The expected cost of energy not served is formulated considering the amount of load shedding (PL^{t}_{sh}) for each possible and credible abnormal operation scenario and the average value of lost load ($Voll_{Ave}$) according to relations (31) and (32).

$$EENS^{t}_{Cost} = Voll_{Ave} \times (\sum_{k=1}^{N_{th}} (\Pr{}^{O,t}_{k} \times PL^{t}_{sh}(k)) + Voll_{Ave} \times (\sum_{Sci=1}^{Sc_n} \rho r_{WTj}{}^{Sci} \times PL^{t}_{sh}(Sci) + \sum_{k=1}^{N_{th}}\sum_{Sci=}^{Sc_n} \Pr{}^{O,t}_{k} \times \rho r_{WTj}{}^{Sci} \times PL^{t}_{sh}(k, Sci)) \quad (31)$$

$$EENS^{t}_{Cost} \le EENS^{t\,\text{arg}et,t}_{Cost} \quad (32)$$

In the second stage, crossover and mutation operators are applied to parents and child chromosomes during the solution process according to Tables (5) and (6), respectively.

Table (5): Crossover operator for two parent chromosomes to produce a pair of child chromosomes in the second stage

SoC^{t}_{EV1}	SoC^{t}_{EV2}	.	SoC^{t}_{EVm}	DR^{t}_{Res}	DR^{t}_{Com}	DR^{t}_{Ind}	DR^{t}_{Agr}
SoC''^{t}_{EV1}	SoC''^{t}_{EV2}	.	SoC''^{t}_{EVm}	DR''^{t}_{Res}	DR''^{t}_{Com}	DR''^{t}_{Ind}	DR''^{t}_{Agr}
↓			↓				
SoC''^{t}_{EV1}	SoC''^{t}_{EV2}	.	SoC^{t}_{EVm}	DR^{t}_{Res}	DR^{t}_{Com}	DR^{t}_{Ind}	DR^{t}_{Agr}
SoC''^{t}_{EV1}	SoC''^{t}_{EV2}	.	SoC^{t}_{EVm}	DR^{t}_{Res}	DR^{t}_{Com}	DR''^{t}_{Ind}	DR''^{t}_{Agr}

Table (6): Mutation operator in the first child chromosome in the second stage

SoC''^{t}_{EV1}	SoC''^{t}_{EV2}	.	SoC^{t}_{EVm}	DR^{t}_{Res}	DR^{t}_{Com}	DR^{t}_{Ind}	DR^{t}_{Agr}
						↓	
SoC''^{t}_{EV1}	SoC''^{t}_{EV2}	.	SoC^{t}_{EVm}	DR^{t}_{Res}	DR'^{t}_{Com}	DR^{t}_{Ind}	DR^{t}_{Agr}

The genetic algorithm solves the second-stage model of the main problem. The total penalty check and the algorithm run again while the convergence condition is satisfied. Finally, the power generation of TUs and WTs, the amount of SR on TUs, the participation of residential, commercial, industrial, and agricultural loads, and the charge-discharge of EV batteries are optimally determined.

V. Numerical Study and Simulation Results

To confirm the efficiency of the proposed model, numerical studies have been applied to IEEE standard test systems with 32 TUs. The peak load is equal to 2850 MW [30]. The generation system has ten thermal power plants. Their technical information comes in Tables (7) and (8). The wind farm has 25 WTs, and each WT is 2 MW. The average and standard deviation of wind speed are 22.46 km/h and 5.7 km/h, respectively. Characteristics of WTs such as cut-out, cut-in, and the nominal wind speed are equal to 40, 5, and 20 km/h,

respectively. Figure (3) shows the power output of wind farms in terms of MW with ARMA time series during a year.

Table (7): TUs Technical information including generation capacity, ramp rate, and forced outage rates

GenCos	Number of units	Pmax	Pmin	RR	λ
Gen1	4	50	0	10	4.42
Gen2	2	400	200	0	7.96
Gen3	1	350	150	9	7.62
Gen4	3	197	80	6	9.22
Gen5	4	155	60	5	9.13
Gen6	3	100	40	3	7.30
Gen7	4	76	25	2	4.47
Gen8	5	12	0	1	2.98
Gen9	4	20	0	4	19.47
Gen10	2	50	0	10	4.47

Figure (8): Technical data on the thermal power plants including coefficients of the cost function

GenCos	α	β	γ
Gen1	0	0.5	0
Gen2	216.576	5.345	0.00028
Gen3	301.233	20.023	0.00300
Gen4	206.703	9.2706	0.00667
Gen5	206.703	9.2706	0.00667
Gen6	216.703	9.2706	0.00667
Gen7	220.703	9.3706	0.00667
Gen8	226.703	9.3706	0.00669
Gen9	236.703	9.4706	0.00668
Gen10	256.703	9.3706	0.00677

Figure (4) shows the hourly load demand of the understudy network for a year. Here, the first day of the year is considered for operation planning.

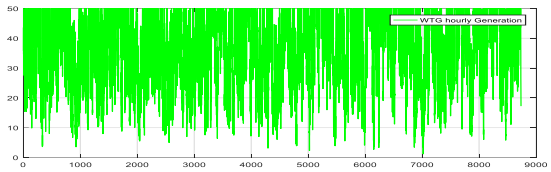

Figure (3): ARMA time series forecast for the power output of WTs

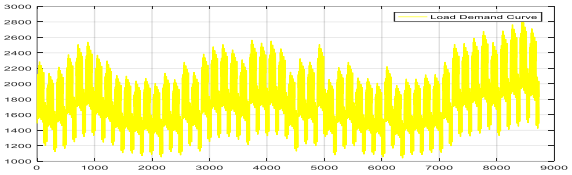

Figure (4): Hourly load demand for understudy test power system

Total load demand includes a fixed part and multiple variable segments. Table (9) gives expected information for residential, commercial, industrial, and agricultural loads in terms of the percentage of peak load, and their constant and maximum consumption is in Table (10).

Table (9): Expected information for residential, commercial, industrial and agricultural loads in terms of the percentage of peak load

D_ExInd	D_ExRes	D_ExCom	D_ExAgr
0.50	0.15	0.15	0.20

Table (10): Constant and maximum consumptions for all types of loads in terms of the percentage of expected load

Loads	D_ExInd	D_ExRes	D_ExCom	D_ExAgr
CBL	0.50	0.70	0.85	0.65
Max	1.5	1.3	1.15	1.35

There are 1000 EVs whose batteries operate in four modes. The minimum and maximum capacity of EV batteries are 5 kW and 25 kW, respectively. We have considered the initial energy stored in batteries equal to their average capacity. The battery charging and discharging efficiencies at the grid-connected state are 0.90 and 0.95, respectively. Inverter efficiency for the battery discharging during moving state is considered 0.85. Each EV consumes 0.15 kWh per kilometer if it travels 80 km/h. We study two cases as below.

- Case study 1: generation system operation planning based on reliability assessment without demand RLs.
- Case Study 2: Generation system operation planning based on reliability assessment with demand RLs.

Code writing of the proposed model is done in MATLAB software that is installed on an ASUS computer with a 2.4 GHz seven-core processor and 8 GB of external memory. Parameters of the genetic algorithm are the initial population of chromosomes, probability of crossover and mutation, and the number of iterations, and their values are equal to 1000, 0.7, 0.3, and 50, respectively.

A. Case study 1: generation system operation planning based on reliability assessment without demand RLs.

This case study loads ED on TUs without demand RLs for a day at the beginning of the year. After running the proposed flowchart, simulation results have been shown in figure (5).

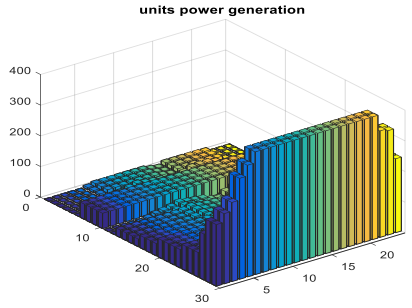

Figure (5): load ED on TUs without RLs for a day at the beginning of the year

Results indicate that the largest and cheapest TUs committed at maximum generation capacity from the first period of operation planning time horizon. In contrast, the most expensive TUs are committed to power generation only for peak hours in the morning and evening during the day. Therefore, TUs can be divided into basic-load, middle-load, and peak-load units considering planned hours. Figures (6) and (7) show the optimal power generation with the cheapest and most expensive units, respectively. Results show that base-load units are continuously committed due to the high start-up cost and are fully dispatched for power generation due to cheaper operation costs. In addition, middle-load and peak-load units provide the SR service due to their high ramp rate characteristics. Figures (8) and (9) show the available and optimal SR capacity on TUs during the day. Figure (9) indicates that maintaining the SR capacity on middle-load and peak-load units without ramp rate consideration cause sub-optimal economic and reliability condition for the power system. ISO must consider balancing conditions between the cost of purchasing SR and the expected cost of energy not served due to SR shortage. Figures (10) and (11) show the simulation results for the total cost of SR provision and the corresponding expected cost of energy not served, respectively.

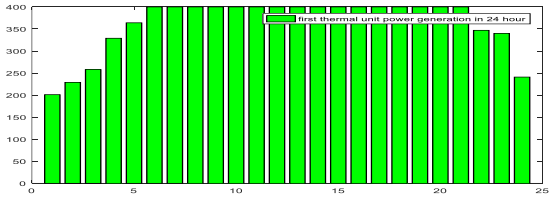

Figure (6): optimal power generation by the largest (cheapest) units

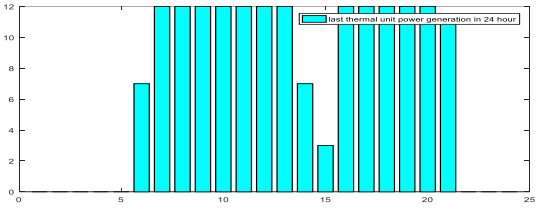

Figure (7): optimal generation by the smallest units (most expensive)

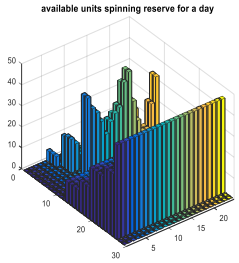

Figure (8): Available SR capacity on TUs

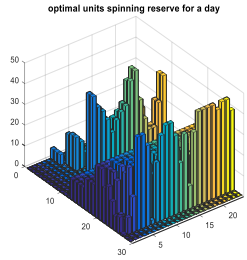

Figure (9): Optimal SR capacity on TUs

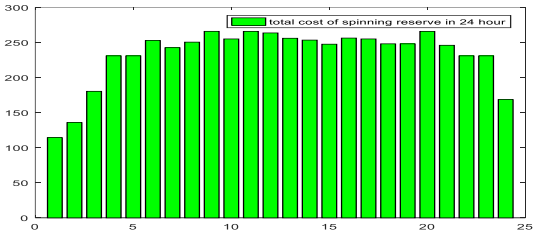

Figure (10): purchasing SR services by TUs

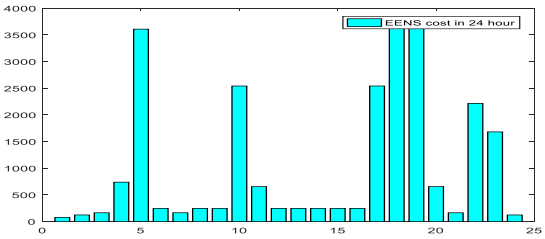

Figure (11): Expected cost of energy not served during a day

The cost of SR provision is variable in the range of 110 dollars to 270 dollars from low load hours to peak hours, but, economic damage due to a shortage of SR in the generation system will get to 3800 dollars in periods 18 and 19 during the day. From the operator's point of view, spending a few hundred dollars for purchasing SR during the operation periods is cost-effective to avoid several thousand dollars in economic damages.

B. Case Study 2: generation system operation planning based on reliability assessment with demand RLs.

This case studies daily operation planning of the generation system based on reliability assessment for a year with demand RLs. Figures (12) and (13) show the simulation results for power generation and SR provision on TUs considering the power generation of WTs and participation of RLs, respectively.

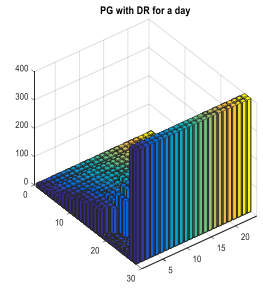

Figure (12): Load ED on TUs considering power generation of WTs and participation of RLs

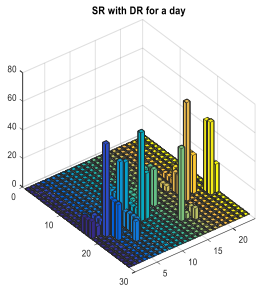

Figure (13): optimal SR on TUs considering power generation of WTs and participation of RLs

Under the new condition, unnecessary start and shutdown of peak-load and middle-load TUs for power generation will decrease, because RLs have a priority right for activation in the power market due to economic and technical issues. In such a way, the SR schedules only on the medium-load TUs. The optimal value of SR is less than the capacity of the largest committed unit and the unit with the most power generation following table (11).

Table (11): optimal SR during a day

t1	**t2**	**t3**	**t4**	**t5**	**t6**
34	21	83	75	63	54
t7	t8	t9	t10	t11	t12
74	96	86	81	32	44
t13	**t14**	**t15**	**t16**	**t17**	**t18**
41	59	51	74	85	95
t19	**t20**	**t21**	**t22**	**t23**	**t24**
105	86	88	22	45	39

In participation of WTs and RLs, simulation results verify that the purchased amount of SR from peak-load and middle-load TUs will drastically reduce due to changes in load profile. Table (12) compares network demand profiles in the presence and absence of RLs. Highlighted parts show that the load demand decreases during peak hours and increases during low-load and medium-load hours with the participation of EVs and other RLs.

Table (12): network demand profile in the presence and absence of RLs

Time	Demand (MW)		Time	Demand (MW)	
	With DR	Without DR		With DR	Without DR
t1	1705.48	1488	t13	1989.04	1998
t2	1739.92	1552	t14	2099	1934
t3	1789.86	1594	t15	2110.04	1913
t4	1895	1743	t16	2103.95	1998
t5	1985	1807	t17	2100.86	2083
t6	2055	1913	t18	1995.16	2126
t7	2063	1956	t19	1994	2126
t8	2055.51	1977	t20	1954.07	2041
t9	2004.57	2019	t21	1945.48	1934
t10	1984.13	2083	t22	1932.31	1764
t11	1931	2041	t23	1920.69	1764
t12	1925	2019	t24	1801.92	1552

Figure (14) shows the participation of residential, commercial, industrial, and agricultural RLs and EVs. The simulation results show that the charge and discharge of the

EV's batteries affect other RLs in the power network. Subsequently, EVs must change their battery charging and discharge depending on different power system conditions following Figure (15). Figure (16) shows the stored energy in EV's batteries during the day. Generally, the participation of EVs and other responsive loads cause to covering the uncertainties of wind turbine power generation, removing unnecessary startup peak-load TUs, and improving power market efficiency.

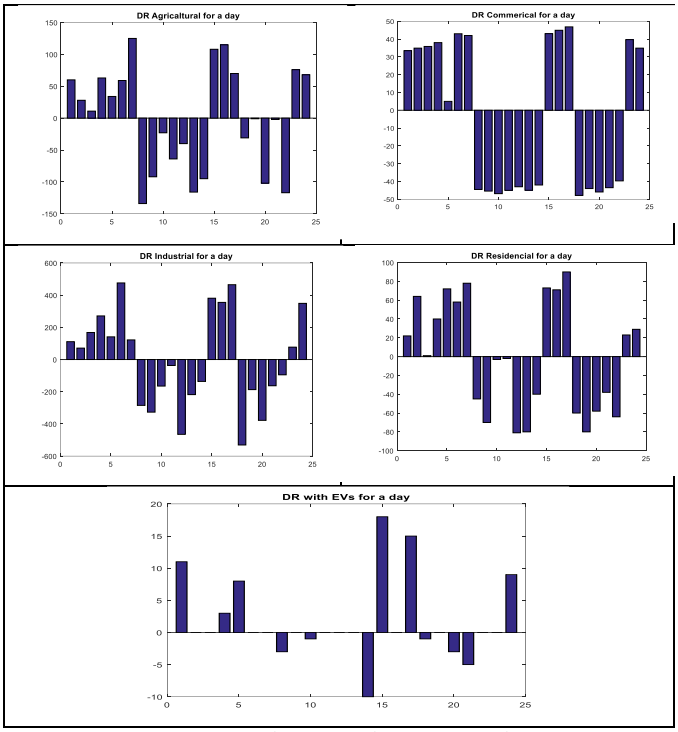

Figure (14): Participation of all types of RLs and EVs for consumption optimization during the day

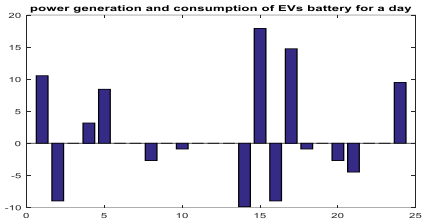

Figure (15): charge and discharge of EV's batteries during the day

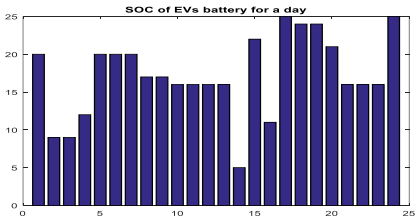

Figure (16): stored energy in EV's batteries during the day

VI. RESULTS COMPARISON

In this section, achieved simulation results for SR and load profile with the proposed reliability-based two-stage model have been compared with the proposed models in [29]. All inputs for the two models are assumed similar, after running their codes, simulation results for comparison of the regulated load profile have been shown in Figures (17).

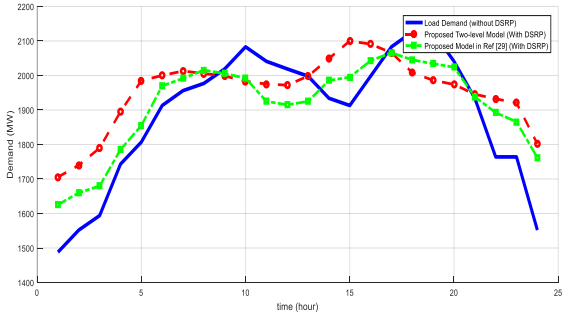

Figure (17): regulated load profile with RLs during the day

As can be seen in figure (17), curves with red and green colors are regulated load profiles using two models, and curve with blue color is the system's daily load profile. Simulation results show that customer's energy demand is properly shifted from peak hours to off-peak and low-load hours using both models. But, the proposed two-stage method can smooth the daily load profile better than the presented model in [29]. Our proposed two-stage model advantage as compared to the model in [29] is the use of cost-benefit analysis to determine the optimal amount of SR in addition to WBA, therefore, there is no overdesign for SR provision on TUs. Under this condition, TUs alongside the WTs can meet the more regulated energy demand of costumer's loads, and also TUs can satisfy the costumer's load point reliability as predefined EENS cost criterion. Figure (18) compares the scheduled SR on TUs in the absence/presence of DSRP using our proposed model and model in reference [29].

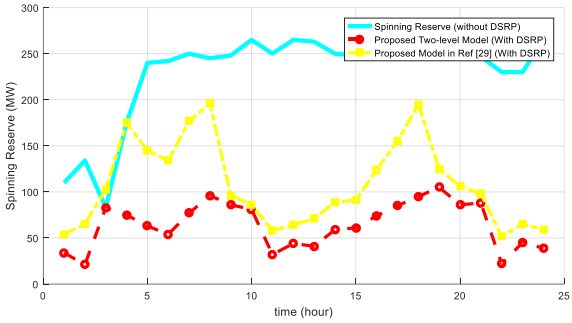

Figure (18): scheduled SR on TUs in absence/presence of DSRP using our proposed model and model in reference [29]

As, the proposed model in [29] only use of WBA, it can determine sub-optimal SR values on TUs based on loss of load probability without consideration of SR provision cost and damage cost due to inadequate SR provision. In the mentioned method, predefined value of customer's reliability is satisfied, but, overdesign can be often seen in hourly SR provision on TUs and EENS cost for power system customers.

VII. CONCLUSION

This paper proposes a new reliability-based model for the ED of thermal-wind units in the participation of RLs on the demand side. Operation planning studies have also been conducted on a test power system with and without DSRP using

responsive loads. The simulation results show that the cheapest TUs are always committed to providing network base load. But, the commitment hours for most expensive TUs are verso and supply the demand during morning and evening peak load hours. Simulation results show that from the operator's point of view, spending a few hundred dollars for purchasing SR during the operation periods is cost-effective to avoid several thousand dollars in economic damages. In addition, the participation of EVs and other RLs cause to cover the power generation uncertainties of WTs and remove unnecessary startup peak-load TUs. Therefore, coordination between WTs and EVs during the operation planning of the generation system provides better economic efficiency for the clearing process of the power market.

References

[1] B. C. Ummels, M. Gibescu, E. Pelgrum, W. L. Kling, A. J. Brand, "Impacts of Wind Power on Thermal Generation Unit Commitment and Dispatch," *IEEE Transactions on Energy Conversion*, March 2007, Vol. 22, No. 1, pp. 44-51.

[2] A. Keane, M. Milligan, C.J. Dent, B. Hasche, C. D'Annunzi, "Capacity Value of Wind Power," *IEEE Transactions on Power Systems*, May 2011, Vol. 26, No. 2, pp. 564 – 572.

[3] X. Zheng, K. Qu, J. Lv, Z. Li, B. Zeng, "Addressing the Conditional and Correlated Wind Power Forecast Errors in Unit Commitment by Distributionally Robust Optimization," *IEEE Transactions on Sustainable Energy*, April 2021, Vol. 12, No. 2, pp. 944 – 954.

[4] N. Zhang, C. Kang, D.S. Kirschen, Q. Xia, W. Xi, and J. Huan, "Planning Pumped Storage Capacity for Wind Power Integration," *IEEE Transactions on Sustainable Energy*, April 2013, Vol. 4, No. 2, pp. 393 – 401.

[5] P. Xiong, and C. Singh, "Optimal Planning of Storage in Power Systems Integrated With Wind Power Generation", *IEEE Transaction on Sustainable Energy*, Jan. 2016, vol. 7, no. 1, pp. 232-240.

[6] A. Nikoobakht, J. Aghaei, M. Shafie-Khah, and J.P.S. Catalão, "Minimizing Wind Power Curtailment Using a Continuous-Time Risk-Based Model of Generating Units and Bulk Energy Storage," *IEEE Transactions on Smart Grid*, Nov. 2020, Vol. 11, No. 6, pp. 4833–4846.

[7] W-M. Lin, C-Y. Yang, M-T. Tsai, and Y-H. Wang, "Unit Commitment with Ancillary Services in a Day-Ahead Power Market," *Applied Science*, 2021, Vol. 11, No. , 12, pp. 1-13.

[8] L. Hao, J. Ji, D. Xie, H. Wang, W. Li, and P. Asaah, "Scenario-based Unit Commitment Optimization for Power System with Large-scale Wind Power Participating in Primary Frequency Regulation," *Journal of Modern Power System and Clean Energy*, Nov. 2020, Vol. 8, No. 6, pp. 1259-1267.

[9] Z. Wang, U. Munawar, and R. Paranjape, "Stochastic Optimization for Residential Demand Response with Unit Commitment and Time of Use," *IEEE Transactions on Industry Applications*, March-April 2021, Vol. 57, No. 2, pp. 1767-1778.

[10] A. Khodaei, M. Shahidehpour and Sh. Bahramirad, "SCUC with Hourly Demand Response Considering Inter temporal Load Characteristics," *IEEE Transaction on Smart Grid*, Sept. 2011, Vol. 2, No. 3, pp. 564-571.

[11] M.E. Honarmand, V. Hosseinnezhad, B. Hayes, M. Shafie-Khah, and P. Siano, "An Overview of Demand Response: From its Origins to the Smart Energy Community," *IEEE Access*, July 2021, Vol. 9, pp. 96851-96876.

[12] M. Raoofat, M. Saad, S. Lefebvre, D. Asber, H. Mehrjedri, and L. Lenoir, "Wind power smoothing using demand response of electric vehicles," Elsevier, *International Journal of Electrical Power & Energy Systems*, July. 2018, Vol. 99, pp. 164-174.

[13] H.U.R. Habib, A. Waqar, M.G. Hussien, A.K. Junejo, M. Jahangiri, R.M. Imran, Y. Kim, and J. Kim, "Analysis of Micro-Grid's Operation Integrated to Renewable Energy and Electric Vehicles in view of Multiple Demand Response Program," *IEEE Access*, Jan. 2022, Vol. 10, pp. 7598-7638.

[14] X. Wang, H. Zhang, S. Zhang, and L. Wu, "Impacts of joint operation of wind power with electric vehicles and demand response in the electricity market," Elsevier, *Electric Power Systems Research*, Dec. 2021, Vol. 201, pp. 1-12.

[15] Y. Li, Z. Ni, T. Zhao, M. Yu, Y. Liu, L. Wu, and Y. Zhao, "Coordinated Scheduling for Improving Uncertain Wind Power Adsorption in Electric Vehicles-Wind Integrated Power Systems by Multi-objective Optimization Approach," *IEEE Transactions on Industry Applications*, June 2020, Vol. 56, No. 3, pp. 2238-2250.

[16]S. F. Syed Vasiyullah, and S. G. Bharathidasan, "Profit Based Unit Commitment of Thermal Units with Renewable Energy and Electric Vehicles in Power Market," Springer, *Journal of Electrical Engineering & Technology*, 2021, Vol. 16, No. 1, pp. 115–129.

[17]J. Wang, Y. Shi, and Y. Zhou, "Intelligent Demand Response for Industrial Energy Management Considering Thermostatically Controlled Loads and EVs," *IEEE Transactions on Industrial Informatics*, June 2019, Vol. 15, No. 6, pp. 3432-3442.

[18] R. Lu, T. Ding, B. Qin, J. Ma, X. Fang, and Z. Dong, "Multi-Stage Stochastic Programming to Joint Economic Dispatch for Energy and Reserve With Uncertain Renewable Energy," *IEEE Transactions on Sustainable Energy*, July 2020, Vol. 11, No. 3, pp. 1140-1151.

[19] C. Zhao, C. Wan, and Y. Song, "Operating Reserve Quantification Using Prediction Intervals of Wind Power: An Integrated Probabilistic Forecasting and Decision Methodology," *IEEE Transactions on Power Systems*, July 2021, Vol. 36, No. 4, pp. 3701-3714.

[20] R. Billinton, and R. Karki, "Capacity reserve assessment using system well-being analysis," *IEEE Transactions on Power Systems*, May 1999, Vol. 14, No. 2, pp. 433 – 438.

[21] H. Dange and R. Billinton, "Effects of wind power on bulk system adequacy evaluation using the Well-being analysis framework", *IEEE Transaction on Power System*, Aug. 2009, vol. 24, no. 3, pp. 1232-1240.

[22] N. Xu and C. Chung, "Uncertainties of EV charging and effects on well-being analysis of generating systems," *Transaction on Power Systems*, 2015, vol. 30, No. 5, pp. 2547–2557.

[23] A. Abdulwhab, and R. Billinton, "Generating System Well-being Index Evaluation", Elsevier, *Electrical Power and Energy Systems*, 2004, Vol. 26, No. 3, pp. 221–229.

[24] W. Wangdee, R. Billinton, "Bulk electric system well-being analysis using sequential Monte Carlo simulation," *Transaction on Power System*, 2006, Vol. 21, pp. 188–193.

[25] M. V. Bhatkar, and A. K. Verma, "Uncertainty Consideration in Power System Well-Being Assessment using Fuzzy Set Approach," Springer, Opsearch, 2008, Vol. 45, pp. 237–248.

[26] D. Kumar Khatod, V. Pant, and J. Sharma, "Analytical Approach for Well-Being Assessment of Small Autonomous Power Systems With Solar and Wind Energy Sources," *IEEE Transactions on Energy Conversion*," June 2010, Vol. 25, No. 2, pp. 535-545.

[27] R. Billinton and B. Karki, "Well-being analysis of wind integrated power systems," *Transaction on Power Systems*, 2011, Vol. 26, No. 4, pp. 2101-2108.

[28] N. Z. Xu, and C. Y. Chung, "Well-Being Analysis of Generating Systems Considering Electric Vehicle Charging," *IEEE Transactions on Power Systems*, Sept. 2014, Vol. 29, No. 5, pp. 2311 – 2320.

[29] B. Liang, W. Liu, F. Wen, and Md. Abdus Salam, "Well-Being Analysis of Power Systems Considering Increasing Deployment of Gas Turbines," *Energies*, July 2017, Vol. 10, pp. 1-18.

[30]C. Grigg, P. Wong, P. Albrecht, R. Allan, M. Bhavaraju, R. Billinton, Q. Chen, C. Fong, S. Haddad and S. Kuruganty, "The IEEE Reliability Test System-1996. A report prepared by the Reliability Test System Task Force of the Application of Probability Methods Subcommittee," 1999, Vol. 14, No. 3, pp. 1010-1020.